



VCU

Virginia Commonwealth University
VCU Scholars Compass

Electrical and Computer Engineering Publications

Dept. of Electrical and Computer Engineering

2006

Infrared absorption in a quantum wire: A technique to measure different types of spin-orbit interaction strengths

S. Bandyopadhyay

Virginia Commonwealth University, sbandy@vcu.edu

S. Sarkar

Virginia Commonwealth University, Jadavpur University

Follow this and additional works at: http://scholarscompass.vcu.edu/egre_pubs

 Part of the [Electrical and Computer Engineering Commons](#)

Bandyopadhyay, S., Sarkar, S. Infrared absorption in a quantum wire: A technique to measure different types of spin-orbit interaction strengths. *Applied Physics Letters*, 88, 183108 (2006). Copyright © 2006 AIP Publishing LLC.

Downloaded from

http://scholarscompass.vcu.edu/egre_pubs/98

This Article is brought to you for free and open access by the Dept. of Electrical and Computer Engineering at VCU Scholars Compass. It has been accepted for inclusion in Electrical and Computer Engineering Publications by an authorized administrator of VCU Scholars Compass. For more information, please contact libcompass@vcu.edu.

Infrared absorption in a quantum wire: A technique to measure different types of spin-orbit interaction strengths

S. Bandyopadhyay^{a)} and S. Sarkar^{b)}

Department of Electrical and Computer Engineering, Virginia Commonwealth University, Richmond, Virginia 23284

(Received 30 August 2005; accepted 29 March 2006; published online 4 May 2006)

We show that the dominant absorption peak due to intersubband transition in a gated quantum wire will split into a main peak and two satellite peaks if *both* Rashba and Dresselhaus spin-orbit interactions are present. One satellite peak will be redshifted, and the other blueshifted. From the relative intensity of either satellite peak, and the magnitude of the red- or blueshift, we can determine *both* Rashba and Dresselhaus interaction strengths *separately*, if we also carry out a Hall measurement to determine the carrier concentration and a quantized conductance step measurement to determine the energy separation between subbands. This method may be a convenient alternative to usual magnetotransport measurements used to measure spin-orbit interaction strengths. It is also more powerful because it allows us to measure the strengths of the two types of interactions separately. © 2006 American Institute of Physics. [DOI: 10.1063/1.2200391]

Measuring the spin-orbit interaction strength in semiconductor materials is an important objective since this interaction forms the basis of many spintronic devices¹ and even quantum computers.² Normally, the interaction strength is measured using magnetotransport techniques, such as beating patterns in Shubnikov–de Haas oscillations.³ Such experiments are difficult, and sometimes inconclusive. First, the material must have a high mobility for the oscillations to be visible at reasonable magnetic field strengths. Second, considerable theoretical analysis is required to extract the strength of the interaction from the beating patterns.³ Finally, such beating patterns need not necessarily originate from spin-orbit interaction at all. In fact, they could be due to magnetointersubband scattering.⁴ In view of all this, there is a demand for alternate unambiguous techniques to measure the spin-orbit interaction strength in materials.

In this letter, we present an alternate technique that can be used to measure the spin-orbit interaction strength in a quantum wire using optical (infrared) absorption, preceded by a simple Hall measurement to determine the carrier concentration. A quantized conductance step experiment^{5,6} will also be necessary to determine the intersubband spacing in energy, as well as to ensure that only the two lowest subbands are occupied by carriers. Our technique is different from other optical techniques such as the circular photogalvanic effect, which can measure spin-orbit interaction strength, but requires monitoring photocurrents.⁷ Therefore, that method is applicable only to materials that have sufficiently long radiative recombination lifetimes to produce enough photocurrent. Our method does not suffer from such shortcomings. Moreover, it allows separate determination of the Rashba and Dresselhaus interaction strengths. We will illustrate our technique for a quantum wire structure.¹

Consider a quantum wire structure defined by split gates on a two-dimensional electron gas (2-DEG), as shown in Fig. 1. The split gates induce a parabolic confinement on the electron gas, forming a quantum wire. We will assume that the quan-

tum wire is in the [100] crystallographic direction. To the lowest order, the energy dispersion relations of spin-split subbands in the quantum wire are given by⁸

$$E_n^\pm = E_\Delta + (n + 1/2)\hbar\omega + (\hbar^2/2m^*)[k^2 \pm 2(m^*/\hbar^2)(\eta^2 + \alpha_n^2)^{1/2}k] = E_n + (\hbar^2/2m^*)[k \pm \kappa_n]^2,$$

$$\kappa_n = (m^*/\hbar^2)(\eta^2 + \alpha_n^2)^{1/2}, \quad (1)$$

$$E_n = E_\Delta + (n + 1/2)\hbar\omega - (\hbar^2/2m^*)\kappa_n^2,$$

where the \pm sign refers to orthogonal-spins. Here, n is the transverse subband index, E_Δ is the confinement energy due to the (usually triangular) confining potential in the direction perpendicular to the heterointerfaces (y direction in Fig. 1), ω is the curvature of the confining potential due to the split gates (i.e., confining potential in the z direction), k is the wave vector along the axis of the wire (along the x direction), m^* is the effective mass, η is the strength of the Rashba interaction, and α_n is the strength of the Dresselhaus interaction in the n th transverse subband. The Rashba interaction is caused by structural inversion asymmetry due to the triangular potential well confining carriers in the plane of the electron gas, while the Dresselhaus interaction is caused by bulk inversion asymmetry in noncentrosymmetric materials. The

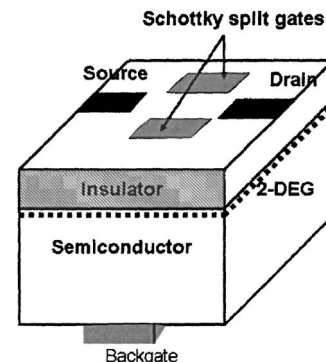


FIG. 1. The quantum wire structure defined by split gates on a two-dimensional electron gas (2-DEG). A backgate is used to vary the carrier concentration in the channel. The quantum wire axis is assumed to be along the [100] crystallographic direction.

^{a)} Author to whom correspondence should be addressed; electronic mail: sbandy@vcu.edu

^{b)} On leave from Department of Electronics and Telecommunication Engineering, Jadavpur University, Kolkata, India.

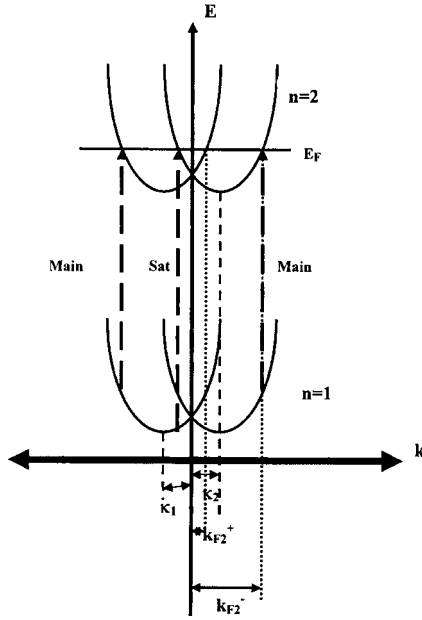


FIG. 2. The energy dispersion of spin split subbands in a quantum wire. The various quantities referred to in the text are shown. We show transitions corresponding to the two main peaks (transitions involving nearly parallel spin states) and a transition corresponding to the blueshifted satellite peak (involving nearly antiparallel spin states). They are labeled “Main” and “Sat.” This diagram is not to scale.

Dresselhaus interaction, unlike the Rashba interaction, depends on the electron wave functions and is therefore different in different subbands.⁸ The dispersion relations are shown schematically in Fig. 2.

The spin eigenstates in two spin-split subbands with the same index n but with orthogonal spins are⁸

$$\psi_n^+ = \phi_n(z) \begin{bmatrix} \cos \theta_n \\ \sin \theta_n \end{bmatrix} e^{ik_n x}, \quad \psi_n^- = \phi_n(z) \begin{bmatrix} \sin \theta_n \\ -\cos \theta_n \end{bmatrix} e^{ik_n x}, \quad (2)$$

$$\theta_n = (1/2)\arctan(\alpha_n/\eta),$$

where $\phi_n(z)$ is the z component of the wave function (simple harmonic oscillator wave function) in the n th subband. Note that θ_n is subband dependent since α_n is subband dependent. As a result, two spin states within the same subband are orthogonal, but within two different subbands are never completely orthogonal since $\theta_p \neq \theta_q$. In other words, the spin quantization axes in different transverse subbands are only *nearly* parallel or *nearly* antiparallel. This is entirely a consequence of the fact that the Dresselhaus interaction is subband dependent.

The intensity of the absorption peak corresponding to excitation from the p th subband to the q th subband is proportional to the square of the overlap between the wave functions in these subbands. Since there are two nondegenerate spin states in each subband, there can be at most $2 \times 2 = 4$ distinct absorption peaks. Two of them will involve transitions between states with nearly parallel spins and the other two between nearly antiparallel spins. These intensities are given by

$$I_{p-}^{q-} = I_{p+}^{q+} = \Xi |\langle \phi_q(z) | \phi_p(z) \rangle|^2 \cos^2(\theta_p - \theta_q), \quad (3)$$

$$I_{p-}^{q+} = I_{p+}^{q-} = \Xi |\langle \phi_q(z) | \phi_p(z) \rangle|^2 \sin^2(\theta_p - \theta_q),$$

where Ξ is some constant. The first line of Eq. (3) corresponds to transitions between nearly parallel spin states and

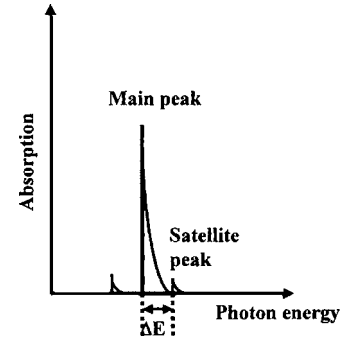


FIG. 3. Schematic representation of the infrared absorption spectra in a quantum wire in the presence of strong Rashba and Dresselhaus spin-orbit interactions. The main peak and the satellite peak heights are not to scale. We show the line shapes corresponding to the $E^{-0.5}$ energy dependence of the density of states in a quantum wire.

the second line between nearly antiparallel spin states. The “nearly parallel” transition gives rise to the main peak and the “nearly antiparallel” transitions cause the satellite peaks because their intensities are much weaker than the main peak intensity when $\theta_p \cong \theta_q$. From Eq. (3), we see that the ratio of the intensity of a satellite peak to that of the main peak is $\tan^2(\theta_p - \theta_q)$. In most cases of interest, such as in InAs wires, the Rashba interaction strength will be much larger than the Dresselhaus interaction strength,³ so that $\alpha_n \ll \eta$. Therefore, $\tan^2(\theta_p - \theta_q) \cong [(\alpha_p - \alpha_q)/2\eta]^2 = [a_{42}m^*\hbar\omega(q-p)/(2\eta\hbar^2)]^2$, where a_{42} is the material constant determining the strength of the Dresselhaus interaction. Consequently, the ratio of the two intensities is

$$\frac{I_{\text{satellite}}}{I_{\text{main}}} = \frac{I_{p-}^{q+}}{I_{p-}^{q-}} = \left[\frac{a_{42}m^*(q-p)\hbar\omega}{2\eta\hbar^2} \right]^2 \quad \text{if } \alpha_n \ll \eta. \quad (4)$$

It is interesting to note that if the Rashba interaction strength $\eta=0$, then $\theta_p = \theta_q = \pi/4$, and the intensity of the satellite peaks is exactly zero. Similarly, if the Dresselhaus interaction is either totally absent or equal in different subbands ($\alpha_p = \alpha_q$), then $\theta_p = \theta_q$, and again the satellite peak intensity is zero. These conditions merely reflect the fact that transitions between strictly antiparallel spin states are forbidden since these states are mutually orthogonal. Therefore, *both* Rashba and Dresselhaus interactions are required, and the Dresselhaus interaction must be *different* in different subbands, in order for the satellite peaks to appear. The variation of spin-orbit interaction among different subbands was also recently shown to give rise to a double peak structure in the optical spectra of quantum cascade lasers.⁹

Let us now consider a quantum wire in which the two lowest subbands are occupied at low temperatures. Occupancy of only the two lowest subbands in a split gate structure can be ensured by using a backgate to vary the carrier concentration in the wire¹⁰ and monitoring the longitudinal resistance. If the quantum wire is sufficiently clean, the conductance will exhibit the well-known quantized steps as the backgate potential is varied.⁵ When only two subbands are occupied, the conductance of the wire will be $\sim 4e^2/h$. The Fermi level E_F will then be located between the second and third subband bottoms, as shown in Fig. 2. Since all states below the Fermi level are filled with electrons, the lowest state to which an electron can be photoexcited is at the Fermi level. Let the Fermi wave vectors in the spin-split second subband be called k_{F2}^+ and k_{F2}^- . Because of spin splitting, $k_{F2}^+ \neq k_{F2}^-$ (see Fig. 2) and the difference between them is $2\kappa_2$.

In a quantum wire, absorptions involving third and higher subbands are increasingly weak since carrier confinement in the higher subbands gets progressively weaker. Therefore, we need to concern ourselves only with the lowest two subbands in calculating the dominant absorption characteristics. The photon frequencies corresponding to transitions between nearly parallel states (main absorption peaks) are given by

$$h\nu_{-}^{2-} = \hbar\omega - (\hbar^2/m^*)k_{F2}^-[\kappa_2 - \kappa_1]; \quad h\nu_{+}^{2+} = \hbar\omega + (\hbar^2/m^*)k_{F2}^+[\kappa_2 - \kappa_1], \quad (5)$$

whereas those due to the “nearly antiparallel” transitions (satellite peaks) are given by

$$h\nu_{-}^{1+} = \hbar\omega + (\hbar^2/m^*)k_{F2}^+(\kappa_1 + \kappa_2); h\nu_{+}^{1-} = \hbar\omega - (\hbar^2/m^*)k_{F2}^-(\kappa_1 + \kappa_2). \quad (6)$$

The frequency shift between the two main peaks is therefore $h\nu_{+}^{2+} - h\nu_{-}^{2-} = (\hbar^2/m^*)[k_{F2}^+ + k_{F2}^-][\kappa_2 - \kappa_1] \approx [k_{F2}^+ + k_{F2}^-](\alpha_2^2 - \alpha_1^2)/2\eta \approx [k_{F2}^+ + k_{F2}^-]a_{42}m^*\omega/(2\hbar\eta)$. We will show later that for reasonable carrier concentrations, this frequency difference is a few μeV in energy. Therefore, thermal broadening at any practical temperature will make the two main peaks overlap and appear as a single peak.

From Eqs. (5) and (6), we see that one satellite peak is *blueshifted* from the main peak by an amount of energy $\Delta E_{\text{blue}} = (\hbar^2/m^*)k_{F2}^+(\kappa_1 + \kappa_2) = k_{F2}^+[(\eta^2 + \alpha_1^2)^{1/2} + (\eta^2 + \alpha_2^2)^{1/2}]$, while the other is redshifted by an amount of energy $\Delta E_{\text{red}} = (\hbar^2/m^*)k_{F2}^-(\kappa_1 + \kappa_2) = k_{F2}^-[(\eta^2 + \alpha_1^2)^{1/2} + (\eta^2 + \alpha_2^2)^{1/2}]$. These shifts depend on k_{F2}^+ and k_{F2}^- .

Since spin splitting is small, $k_{F2}^+ \cong k_{F2}^- = k_{F2}$. The question now is how do we know k_{F2} ? This requires performing a Hall measurement to determine the total carrier concentration n_l in the quantum wire. Let k_{F1} be the Fermi wave vector in the first subband, i.e., k_{F1} is the wavevector where the first subband parabola intersects the Fermi level E_F . The two horizontally displaced parabolas in the first subband will intersect the Fermi level at slightly different wave vectors, but we will ignore that difference since the spin splitting is small. The carrier concentration in the first subband is then $n_{l1} = 2(k_{F1} - \kappa_1)/\pi$, while in the second subband it is $n_{l2} = 2(k_{F2} - \kappa_2)/\pi$.

From the dispersion relations (Fig. 2), we see that $(\hbar^2/2m^*)(k_{F1} - \kappa_1)^2 = \hbar\omega + (\hbar^2/2m^*)(k_{F2} - \kappa_2)^2$. Therefore the total carrier concentration is $n_l = n_{l1} + n_{l2} = 2\{(2m^*/\hbar^2)[\hbar\omega + (\hbar^2/2m^*)(k_{F2} - \kappa_2)^2]\}^{1/2}/\pi + 2\pi(k_{F2} - \kappa_2)/\pi$.

We will consider a material such as InAs, where the Rashba interaction is overwhelmingly dominant over the Dresselhaus interaction.³ Therefore, $\kappa_2 \cong (m/\hbar^2)\eta$. Consequently, the total carrier concentration can be written as

$$n_l = n_{l1} + n_{l2} \approx 2\left\{\frac{2m^*}{\hbar^2}\left[\hbar\omega + \frac{\hbar^2}{2m^*}(k_{F2} - m^*\eta/\hbar^2)^2\right]\right\}^{1/2}/\pi + 2(k_{F2} - m^*\eta/\hbar^2)/\pi. \quad (7)$$

Similarly, if the Rashba interaction is dominant, then the red- and blueshifts can be rewritten as

$$\Delta E_{\text{blue}} = \Delta E_{\text{red}} \approx 2k_{F2}\eta. \quad (8)$$

Equations (4), (7), and (8) are three equations with four unknowns: a_{42} (the strength of the Dresselhaus interaction), η (the strength of the Rashba interaction), k_{F2} , and $\hbar\omega$. The last quantity can be found from quantized conductance step measurements.^{5,6} Therefore, solutions of the three simulta-

neous equations with three unknowns allow us to determine the strengths of the Rashba and Dresselhaus interaction strengths— η and a_{42} —separately.

We now proceed to estimate the magnitude of the red- or blueshifts ΔE in order to examine if it is observable under normal conditions. Typically, $\eta \sim 10^{-11}$ eV m in materials such as InAs (Ref. 3) and $\hbar\omega = 10$ meV.⁶ Note that in order for $(k_{F2} - \kappa_2)$ to be positive, $n_l > 2(2m^*\omega/\hbar)^{1/2}/\pi = 5.6 \times 10^7/\text{m}$ in InAs. That means this is the minimum carrier concentration required for two subbands to be occupied. Let us assume $n_l \sim 10^8/\text{m}$ (this can be adjusted by the backgate). This yields $k_F \sim 1.57 \times 10^8 \text{ m}^{-1}$. Therefore, Eq. (8) yields that $\Delta E_{\text{blue}} = \Delta E_{\text{red}} \sim 1.57$ meV. Infrared spectral line-widths of 1.2 meV in GaAs quantum wires at a temperature of 8 K have been reported in Ref. 11. Thus, the broadening of the main peak will not interfere with the satellite peak, and the blue- or redshift will be measurable.

Finally, we need to estimate the relative height of the satellite peak with respect to the main peak in order to assess whether it will be above the noise floor. Equation (4) gives this relative height. The quantity a_{42} was calculated to be 7×10^{-29} eV m³ iAs.¹² Using this value, we determine that the ratio of the heights of the satellite peak and the main peak is $\sim 0.02\%$, which should be above the noise floor in low temperature measurements. Thus, we believe that the effect predicted in this letter is observable at low temperatures.

In conclusion, we have shown that the simultaneous presence of Rashba and Dresselhaus interactions in a quantum wire splits the dominant infrared absorption peak into a main peak and two satellite peaks (Fig. 3). The main peak is also slightly split, but from Eq. (5), this splitting is $\sim 4(k_{F2}/\eta)[a_{42}m^*\hbar\omega/(\hbar^2)]^2 \sim 0.4 \mu\text{eV}$, which is not resolvable. The blue- or redshifts of the satellite peaks, and their relative intensities, allow us to determine the Rashba and Dresselhaus spin-orbit interaction strengths separately, if we carry out a Hall measurement and a quantized conductance step measurement to determine the carrier concentration and the subband spacing in energy.

¹S. Datta and B. Das, Appl. Phys. Lett. **56**, 665 (1990); S. Bandyopadhyay and M. Cahay, *ibid.* **85**, 1814 (2004).

²S. Bandyopadhyay, Phys. Rev. B **61**, 13813 (2000).

³B. Das, S. Datta, and R. Reifenberger, Phys. Rev. B **41**, 8278 (1990); J. Nitta, T. Akazaki, H. Takayanagi, and T. Enoki, Phys. Rev. Lett. **78**, 1335 (1997).

⁴N. Tang, S. Shen, Z. W. Zhang, J. Liu, D. J. Chen, J. Lu, R. Zhang, Y. Shi, Y. D. Zhang, Y. S. Gui, C. P. Jiang, Z. J. Qui, S. L. Guo, J. H. Chu, K. Hoshino, T. Someya, and Y. Ayakawa, J. Appl. Phys. **94**, 5420 (2003).

⁵B. J. van Wees, H. van Houten, C. W. J. Beenakker, J. G. Williamson, L. P. Kouwenhoven, D. van der Marel, and C. T. Foxon, Phys. Rev. Lett. **60**, 848 (1988).

⁶G. L. Snider, M. S. Miller, M. J. Rooks, and E. L. Hu, Appl. Phys. Lett. **59**, 2727 (1991); S. J. Koester, C. R. Bolognesi, E. L. Hu, H. Kroemer, M. J. Rooks, and G. L. Snider, J. Vac. Sci. Technol. B **11**, 2528 (1993).

⁷S. D. Ganichev, E. L. Iuchenko, S. N. Danilov, J. Evans, W. Wegscheider, D. Weiss, and W. Prahl, Phys. Rev. Lett. **86**, 4358 (2001); S. D. Ganichev, V. V. Bel'kov, L. E. Golub, E. L. Ivchenko, P. Schneider, S. Giglberger, J. Evans, J. DeBoeck, G. Borghs, W. Wegscheider, D. Weiss, and W. Prahl, Phys. Rev. Lett. **92**, 256 (2004).

⁸S. Bandyopadhyay, S. Pramanik, and M. Cahay, Superlattices Microstruct. **35**, 67 (2004).

⁹V. M. Apalkov, A. Bagga, and T. Chakraborty, e-print cond-mat/0508473.

¹⁰B. Das, M. R. Melloch, and S. Bandyopadhyay, J. Phys.: Condens. Matter **12**, L35 (2000).

¹¹W. Hansen, M. Horst, J. P. Kotthaus, U. Merkt, C. Sikorski, and K. Ploog, Phys. Rev. Lett. **58**, 2586 (1987).

¹²N. Knapp, Phys. Rev. B **53**, 3912 (1996).